Supplementary materials

Atmospheric Concentration of Black Carbon over Africa: Hotspot Regions, Seasonal Dynamics and Future Projections from Bias-Adjusted AerChemMIP Models

Matthews Nyasulu[1], Yan-Lin Zhang[1, 2]*, Cao Fang[1,2], Md. Mozammel Haque[1,2]

[1]School of Ecology and Applied Meteorology, Nanjing University of Information Science and Technology, Nanjing,210044, China.

[2]Atmospheric Environment Canter, Joint Laboratory for International Cooperation on Climate and Environmental Change, Ministry of Education, Nanjing University of Information Science and Technology, Nanjing, 210044, China

Corresponding author: Yan-Lin Zhang (dryanlinzhang@outlook.com, zhangyanlin@nuist.edu.cn).

S1. Potential Source Contribution Function

The PSCF values describe the conditional probability that the trajectories passing through the cells are the major transporters of the pollutants detected at the receptor site (Ashbaugh, 1985). We used trajectory statistical (TrajStat) software to compute the PSCF (Wang et al., 2009). The input meteorological fields were obtained from the Global Data Assimilation System (GDAS). To compute PSCF, the region surrounding the tracking site was divided into small grid cells (ij). The number of end points for the same cell having arrival times at the tracking site to BC concentration higher than an arbitrarily set criterion was defined as $m_{ij.}$ The number of end points that fell in the ijth cell was defined as n_{ij}. PSCF was then calculated as the number of end points for the same cell having arrival times at the sampling site to BC concentration higher than an arbitrarily set criterion divided by the number of trajectory end points passing through the same ijth cell, mathematically expressed as;

$$\mathrm{PSCF_{ij}} = \frac{\mathrm{m_{ij}}}{\mathrm{n_{ij}}} \tag{S3}$$

i and j represent the latitude and longitude in the ijth cell, respectively. The average concentration of BC during the sampling period was considered as the criterion value. There is, however more statistical stability for high values of PSCF as compared to small values (Wang et al., 2009). In order to reduce the effect of smaller values, PSCF values were hence multiplied by a weighted function $w(n_{ij})$ to better reflect the uncertainties in the grid cells. PSCF was therefore described by weighted function as;

$$\mathrm{WPSCF_{ij}} = \mathrm{w(n_{ij})} \times \frac{\mathrm{m_{ij}}}{\mathrm{n_{ij}}} \tag{S4}$$

The weighted function $w(n_{ij})$ was defined as:

$$\mathrm{w(n_{ij})}\begin{cases} 1.00 & \mathrm{n_{ij} > 2n_{ave}} \\ 0.70 & \mathrm{n_{ave} < n_{ij} \leq 2n_{ave}} \\ 0.42 & \mathrm{0.5n_{ave} < n_{ij} \leq n_{ave}} \\ 0.05 & \mathrm{n_{ij} \leq \ 0.5n_{ave}} \end{cases} \tag{S5}$$

n_{ave} is the average endpoints per cell. In this study, high values of WPSCF signified the high probability of the source location of BC, while low values signified low probability of BC source location detected at the receptor site. The above approach has been preferred by several studies to locate the potential source of various pollutants in different environments (Bao et al., 2017; Zhu et al., 2017; Punsompong and Chantara. 2018; Ding et al., 2019; Bilal et al., 2021).

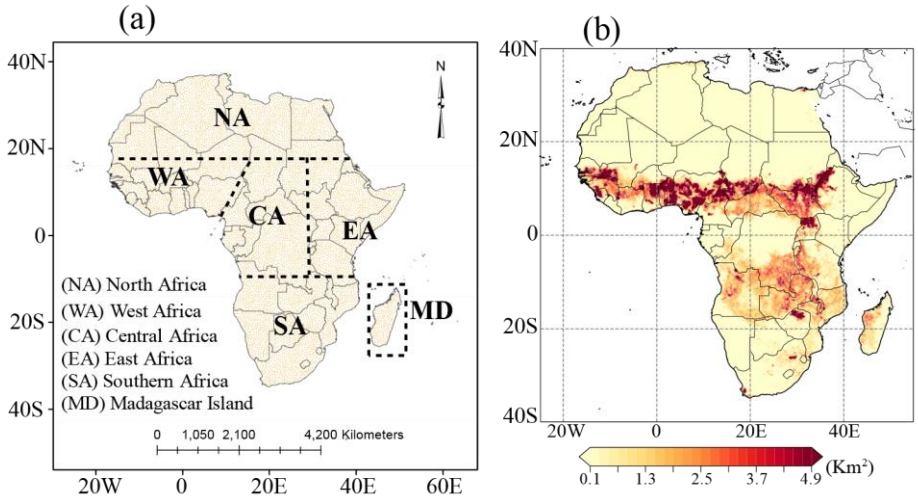

Figure S1. The map of Africa with the sub-divided regions represented by the dotted polygons (a) and the spatial distribution of annual banned area due to forest fires and total annual burned areas based on Global Fire Emission Database (GFED5) (b).

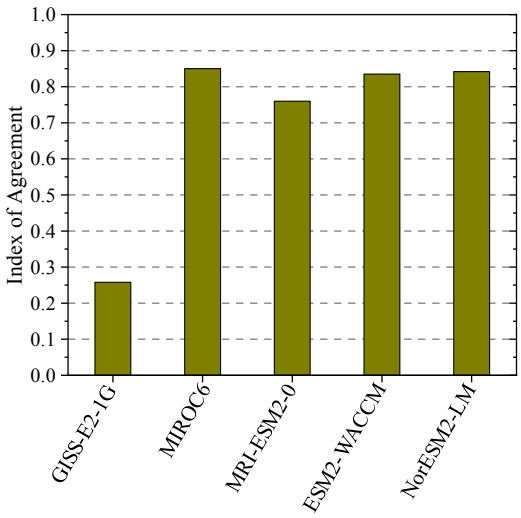

Figure S2. Performance of the individual models based on Index of Agreement against MERRA2 reanalysis.

Table S1. Pairwise comparison of MERRA-2, bias-adjusted multi-model mean (MMM), and unadjusted MMM based on ANOVA post-hoc analysis. A p-value < 0.05 indicates a statistically significant difference (rejection of the null hypothesis), whereas p-value ⩾ 0.05 indicates no significant difference.

Comparison	Mean difference	p-values	Reject
Bias- adjusted MMM *vs* Unadjusted MMM	0.06	0.008	True
Bias- adjusted MMM *vs* MERRA2	-0.02	0.256	False
Unadjusted MMM *vs* MERRA2	-0.09	0.000	True

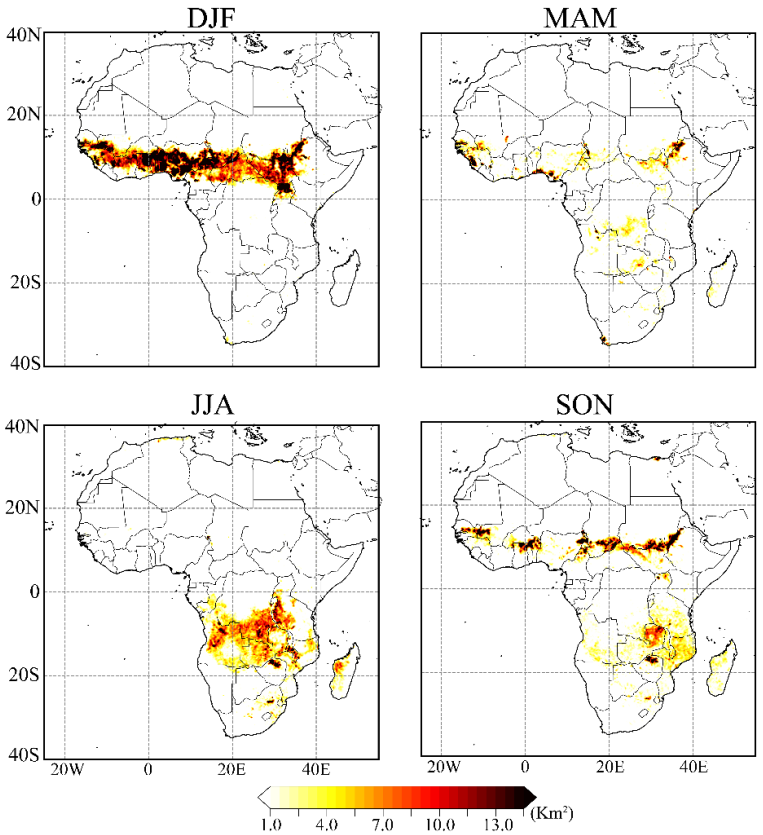

Figure S3. Seasonal spatial distribution of burned area across Africa for DJF, MAM, JJA and SON between 2000 and 2023 based on Global Fire Emission Database (GFED5).

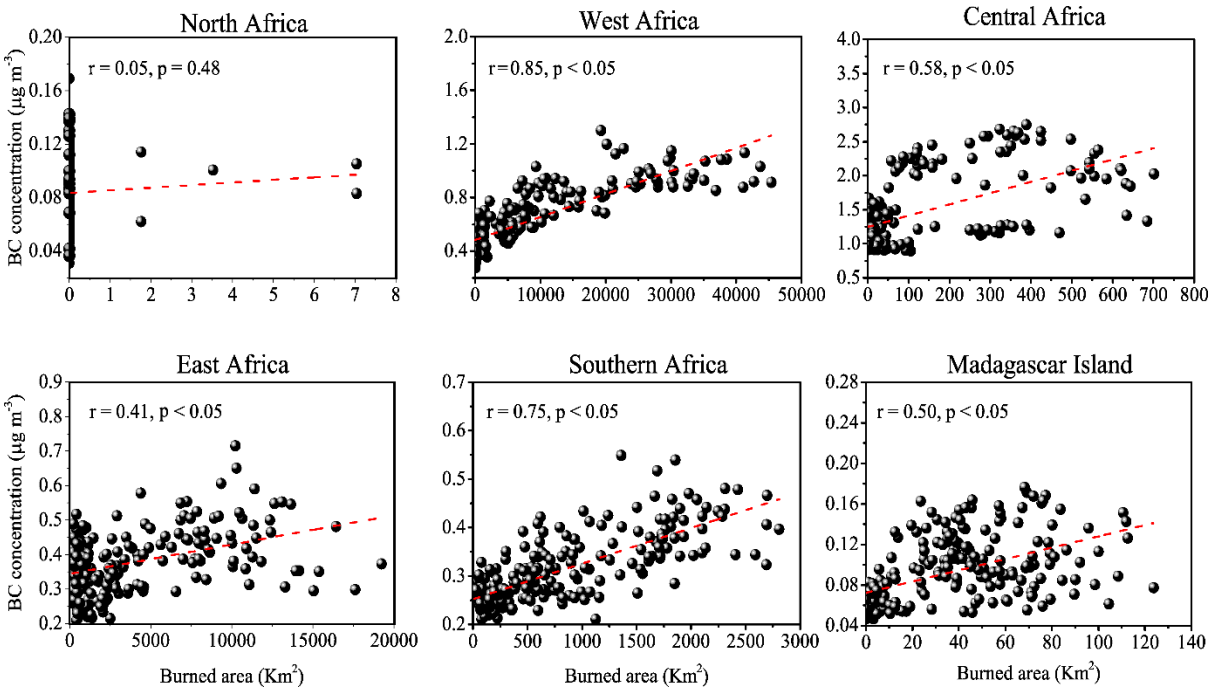

Figure S4. The scatter plots showing relationship between BC and regional total burned area for all the selected regions over the domain.

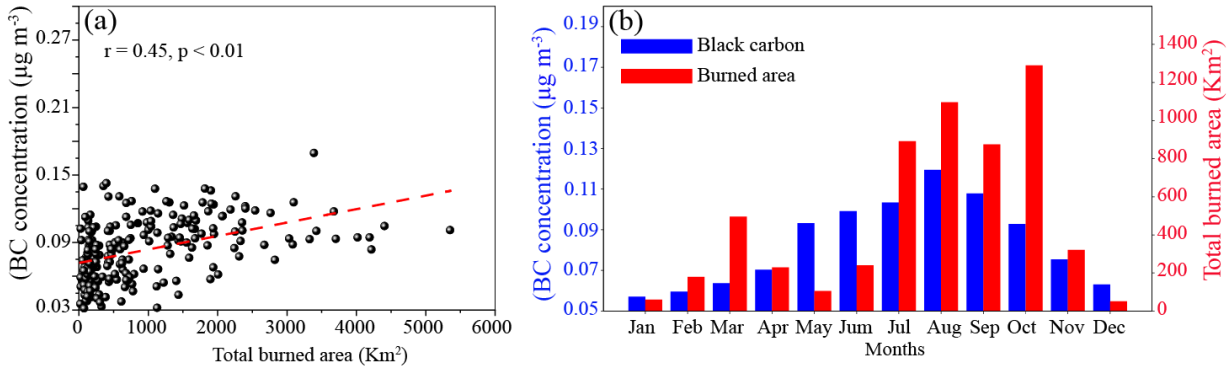

Figure S5. Relationship between (a) North African BC concentration and Europe burned area and (b) the corresponding monthly variation.

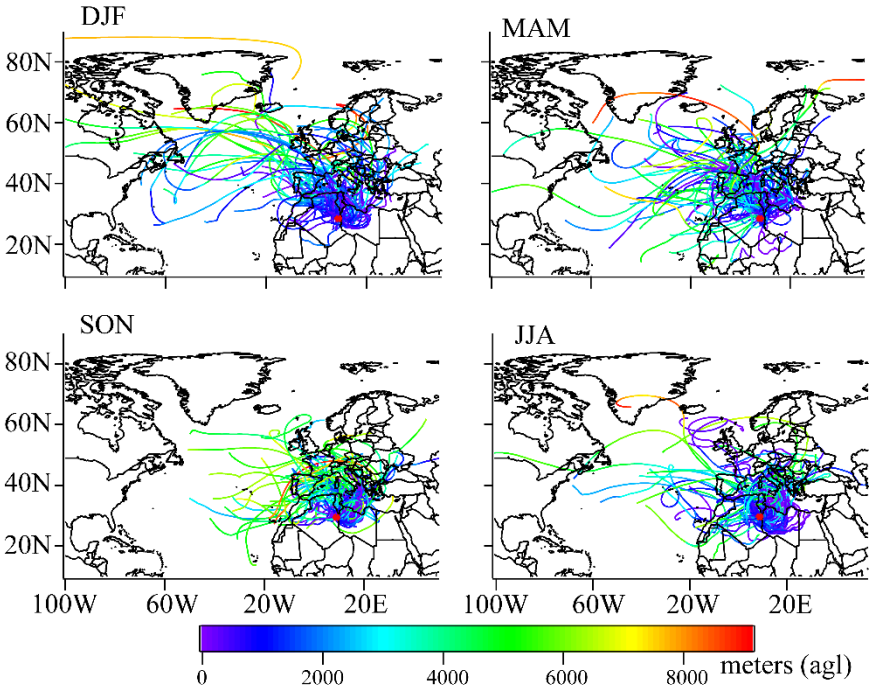

Figure S6. Airmass trajectories arriving over the observation point (shown by red dot) at different altitude above ground level (agl) between January and December of 2023.

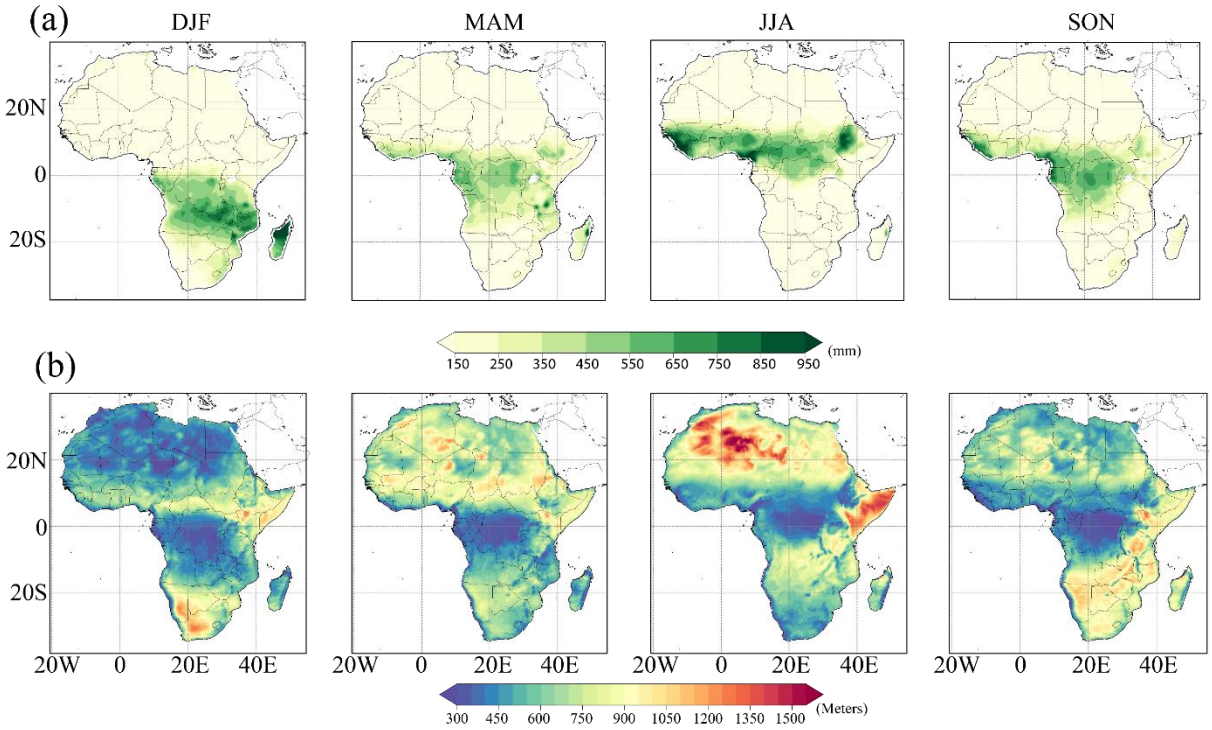

Figure S7. Seasonal distribution of (a), total annual rainfall and (b) atmospheric boundary layer height over Africa.

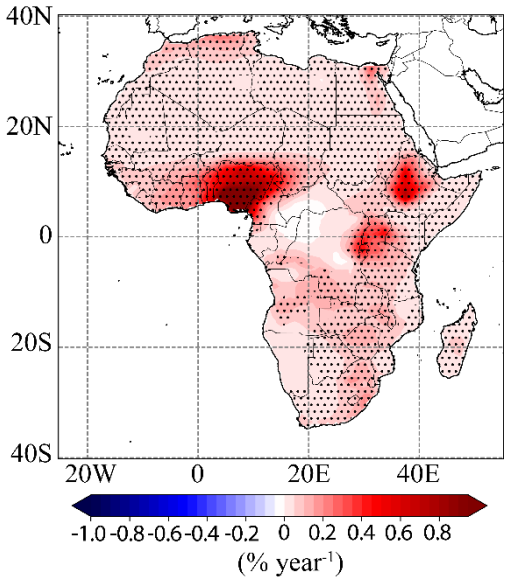

Figure S8. The spatial distribution of BC trends based on Sen's slope and MK trend test between 1980 and 2023. Black dots indicate trends are significant at 0.05 significance level.

85

References

Ashbaugh, L. L., Malm, W. C., and Sadeh, W. Z.: A residence time probability analysis of sulfur concentrations at grand Canyon National Park, Atmospheric Environment, 19(8), 1263–1270. https://doi.org/10.1016/0004-6981(85)90256-2, 1985.

Bao, M., Cao, F., Chang, Y., Zhang, Y. L., Gao, Y., Liu, X., and Zhang, G.: Characteristics and origins of air pollutants and carbonaceous aerosols during wintertime haze episodes at a rural site in the Yangtze River Delta, China, Atmospheric Pollution Research, 8(5), 900–911. https://doi.org/10.1016/j.apr.2017.03.001, 2017.

Bilal, M., Mhawish, A., Nichol, J. E., Qiu, Z., Nazeer, M., Ali, M. A., … Ke, S.: Air pollution scenario over Pakistan: Characterization and ranking of extremely polluted cities using long-term concentrations of aerosols and trace gases, Remote Sensing of Environment, 264(July), 112617. https://doi.org/10.1016/j.rse.2021.112617, 2021.

Ding, H., Kumar, K. R., Boiyo, R., and Zhao, T.: The relationships between surface-column aerosol concentrations and meteorological factors observed at major cities in the Yangtze River Delta, China, Environtal Science Pollution Research, 26(36), 36568–36588. https://doi.org/10.1007/s11356-019-06730-6, 2019.

Punsompong, P., and Chantara, S.: Identification of potential sources of PM10 pollution from biomass burning in northern Thailand using statistical analysis of trajectories, Atmospheric Pollution Research, 9(6), 1038–1051. https://doi.org/10.1016/j.apr.2018.04.003, 2018.

Wang, Y. Q., Zhang, X. Y., and Draxler, R. R.: TrajStat: GIS-based software that uses various trajectory statistical analysis methods to identify potential sources from long-term air pollution measurement data, Environtal Modeling Softw, 24(8), 938–939. https://doi.org/10.1016/j.envsoft.2009.01.004, 2009.

Zhu, Y., Yang, L., Kawamura, K., Chen, J., Ono, K., Wang, X., … Wang, W.: Contributions and source identification of biogenic and anthropogenic hydrocarbons to secondary organic aerosols at Mt. Tai in 2014, Environtal Pollution, 220, 863–872. https://doi.org/10.1016/j.envpol.2016.10.070, 2017.